LINEAR ELECTRICAL PROPERTIES OF PASSIVE AND ACTIVE CURRENTS IN SPHERICAL HEART CELL CLUSTERS

R. T. MATHIAS, *Department of Physiology, Rush Medical College, Chicago, Illinois 60612*

L. EBIHARA, M. LIEBERMAN, AND EDWARD A. JOHNSON, *Department of Physiology, Duke University, Durham, North Carolina 27710*

ABSTRACT Impedance studies were performed on small spherical clusters of embryonic chick heart cells grown in tissue culture. Each syncytial cluster was impaled with two microelectrodes; one injected low amplitude stochastic current and the other recorded the resulting perturbation of intracellular potential. The current and potential records were digitized, decomposed into their sinusoidal components, and the frequency domain impedance of the cluster was determined. The impedance data were compared with a theory for current flow in a spherical syncytium and values were derived for parameters describing the membranes and intercellular clefts of the tissue. The clusters were spontaneously active but usually became temporarily quiescent when impaled with two electrodes. The potential stabilized at a value close to -30 mV. At this depolarized potential, active slow currents, presumably present in the cardiac action potential, contributed noticeably to the linear impedance, producing a resonant peak in the magnitude of the impedance at a frequency of 1–3 Hz. The linearized impedance functions for these currents were characterized in the presence and absence of tetrodotoxin (TTX) and D-600. TTX had no noticeable effect on the impedance but D-600 essentially abolished the active currents. Although the ionic basis of these currents is not known, frequency domain analysis appears to be a viable technique for studying slow currents in heart muscle.

INTRODUCTION

In their attempts to apply the voltage-clamp technique to study the mechanism of the cardiac action potential, electrophysiologists have used a variety of techniques to overcome some of the limitations imposed by the complex geometry of cardiac muscle. Colatsky and Tsien (1979) chose a naturally occurring strand of cardiac muscle that in electron and light microscopic studies had been found to have a relatively simple structure (Johnson and Sommer, 1967). The individual fibers were without a transverse tubular system and, except where they formed junctional complexes with one another, the fibers appeared to be loosely packed, the intercellular spaces being > 1 μm in width. Lee et al. (1979) used a voltage-clamp technique in which a single suction pipette was used to inject current and to measure potential in a single isolated cardiac muscle cell. Morad and Salama (1979) used optical probes to measure and clamp the average potential across all the membranes in a preparation. Other laboratories have tissue-cultured heart muscle into geometries more suitable for the use of the two-microelectrode technique of voltage-clamp (Lieberman et al., 1976; Nathan and DeHaan, 1979). Each method has its own set of artifacts and problems, and each technique

must rely on independent measurements to estimate the degree of actual spatial control of potential.

One independent technique of estimating the suitability of a preparation for voltage-clamp analysis is to study its structure as seen in the electron microscope. Although this is an essential first step, it is not sufficient to determine unequivocally the pathways of electric current in a tissue of complex geometry (Eisenberg and Mathias, 1980). Electron microscopy enables one to identify the probable paths of current flow, but because each path will have a specific resistivity, capacitance, etc., electron microscopy cannot determine quantitatively the importance of each path. To do this, a mathematical model must be constructed that includes the pathways for current flow visualized in electron micrographs. The quantitative importance of each path can then be tested by injecting low levels of current into the preparation and measuring the resulting linear displacement of intracellular potential.

The present paper describes such an analysis performed on spherical clusters of chick heart cells in tissue culture. The mathematical model employed is that of an electrical syncytium of spherical shape (Eisenberg et al., 1979). The experimental protocol was to measure the displacement in intracellular potential induced by small sinusoidal currents of varying angular frequency. Because the pattern of current flow within an aggregate is quite different at the different frequencies of injected current, one can thereby distinguish the electrical parameters that separately describe the surface and inner membranes as well as the inner and extracellular space.

Similar analyses have been performed by Falk and Fatt (1964), Schneider (1970), and Valdiosera et al. (1974) on skeletal muscles, and by Mathias et al. (1979) on the crystalline lens of the eye. One important difference in the analysis described here is in the model of a unit area of membrane. Impedance data from skeletal muscle and the lens are accurately described by a model in which all membranes behave as an ideal resistance in parallel with an ideal capacitance. In heart cell clusters with an average stable potential of -28 mV, the membrane behavior was found to be more complex. The impedance data showed a resonance at a frequency of ~ 2 Hz, which for small perturbations in membrane potential was shown to be linear, but undoubtedly arose from nonlinear, potential- and time-dependent ionic currents. Such currents do not have a simple circuit analog such as a conductance (Chandler et al., 1962; Fishman et al., 1979). Indeed, the data were found to be satisfactorily described by including two potential- and time-dependent processes, or "gates," in the equivalent electrical circuit of the membrane. Although the voltage dependence of these processes was not studied here, the results suggest that linear impedance analysis at different holding potentials might be a useful technique for analyzing such nonlinear currents in heart muscle.

METHODS

Tissue Culture

Clusters of cardiac muscle cells were obtained by the culture techniques described by Ebihara et al. (1980). In brief, the hearts of 11-d-old embryonic chicks were minced and suspended in Ca-Mg-free Hanks' balanced salt solution containing 0.05% trypsin at 37°C. Agitation and gentle pipetting was used to separate the cells. At intervals of 8 min, the entire enzyme solution containing free cells was drawn off and immediately added to an equal volume of cold medium. After completion of the disaggregation, the cells were filtered through multiple layers of gauze and centrifuged. The cell pellet was resuspended in

cold culture medium (55% medium 199, 41% Earle's balanced salt solution, 2% heat-inactivated fetal calf serum, and 2% chick embryo extract). A cell count was made with a hemocytometer, the suspension was appropriately diluted, and 1-ml aliquots were plated into culture dishes containing 4 ml of culture medium. After a 1-h period of incubation at 37°C, the supernate of muscle-enriched cells was used to seed agar-coated culture dishes containing small openings (20 μm) formed on the agar surface by a needle. The cultures were incubated 3–7 d at 37°C in a humidified chamber containing 4% CO_2 and 96% air. To prevent evaporation of the culture medium, an overlay of light mineral oil was added to the culture dishes selected for electrophysiological analysis.

Electron Microscopy

Cultured clusters were prepared for ultrastructural and stereologic analysis by a modification of the methods reported by Horres et al. (1977). The preparations were rinsed four times in medium 199 (37°C) and then fixed for 15 min in 0.83% glutaraldehyde buffered to pH 7.6 with sodium phosphate (280 mosmol/kg). Fixative was removed by rinsing three times with medium 199 and then placing the preparations in cold (0–4°C) 1% cacodylate-buffered osmium tetroxide for 30 min. After rinsing with cacodylate buffer, the preparations were exposed for 10 min to a saturated aqueous solution of thiocarbohydrazide (room temperature) and rinsed again with buffer. A second incubation with cold osmium tetroxide was followed by dehydration in graded ethanols before embedding in epon 812. Thin sections were cut with a diamond knife and mounted on 300-mesh copper grids. The sections were then stained with 1% uranyl acetate for 10 min and examined with an electron microscope (AEI Scientific Instruments, Kratos, Inc., San Diego, Calif.).

Four preparations, ranging in diameter from 50 to 137 μm, were fixed immediately after the experiment and prepared for sectioning according to the methods described above. Measurements of the volume fraction of extracellular space V_e/V_T, membrane surface area/volume of tissue ratio (S_m/V_T), and the ratio of closely apposed (< 300 nm) to not closely apposed cell membrane were made in 17 sections from these four preparations by standard morphometric and stereological techniques (cf. Horres et al., 1977). We obtained these sections by cutting thick sections (1 μm), beginning at the edge of the preparation, and at various distances (relative to the midpoint of the preparation) making thin sections (60–80 nm). In this way the thin sections sampled the cross-sectional profile of a given preparation, thereby allowing us to monitor possible differences in surface-to-volume ratio S_m/V_T with depth of the cells from the surface.

Electrophysiology

Culture dishes were transferred to the heated stage (37°C) of an inverted microscope (Nikon Inc., Instrument Div., Garden City, N.Y., model M) and a gassing ring positioned around the dish to provide an atmosphere of 95% air and 5% CO_2 to maintain the pH at ~ 7.4. Actively contracting clusters of approximately spherical shape were selected for experimentation. The diameter varied considerably from cluster to cluster but no effort was made to select a particular size. We estimated the diameters by looking down on the cluster through a micrometer eyepiece. Because of variation in the vertical shape, the accuracy of this measurement was probably no better than 10%. Each cluster was impaled with two glass microelectrodes, both filled with 3 M K-acetate. The initial resistance of the microelectrodes ranged from 20 Ω to 45 MΩ. The circuits used initially to interface the microelectrodes with standard amplifiers and electronics are described in Mathias et al. (1979). In later experiments, the feedback follower circuit was modified to allow measurement of current as well as potential (Mathias et al., 1981). Both the potential and current electrodes were painted with conductive silver paint (High Purity Silver Paint, SPI Supplies Div. of Structure Probe Inc., Westchester, Pa.). down to within 100 μm of the tip; an insulating coat of varnish (Pearly Pink or Clear, Helena Rubinstein; Red GLPT Insulating Varnish, GC Electronics Div. of Hydrometals, Inc., Rockford, Ill.) was applied over the conductive paint and the time constant of the resulting electrode/interface circuitry was ~ 10 μs. The small delay introduced by this time constant was measured and removed from the data as illustrated in Mathias et al. (1979).

Wide-band stochastic current noise was injected into the clusters from a noise generator (Hewlett-

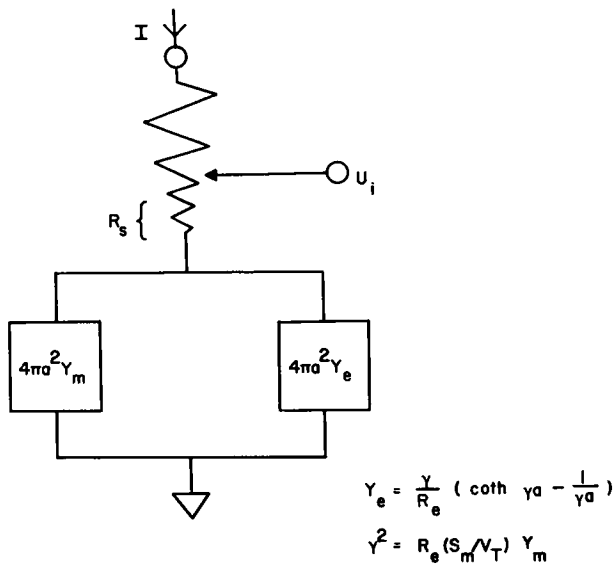

FIGURE 1 The equivalent circuit used to describe the experimental impedance data from heart cell clusters. The specific membrane admittance, Y_m, is described in Eq. 2 of the text. The resistance, R_s, represents the diminishing cross-sectional area of the path for current flow as one approaches a point source. Current injected at the upper terminal of this circuit divides into two parallel paths: one represents the direct path from cell to cell, through intracellular space to and through the surface membranes, given by $4\pi a^2 Y_m$ (note that a is the radius of the spherical aggregate); the other path represents that through the membranes of closely apposed cells and along clefts of extracellular space within the preparation, given by the distributed extracellular admittance, Y_e. The effective extracellular resistivity is represented by the parameter, R_e, which is an effective paramter because it includes the volume fraction of the extracellular space as well as effects of tortuous paths for extracellular current flow, $R_e = \rho_e/(\tau V_e/V_T)$. V_e/V_T is the volume of extracellular space per unit volume of tissue; ρ_e is the specific resistivity of the extracellular solution. The tortuosity factor, τ, depends on many factors but in an isotropic, three-dimensional syncytium, it should approach 2/3 because an average cleft channels current in two of three possible orientations.

Packard Co., Palo Alto, Calif., model 3722A). The input current signal and potential response were separated into their sinusoidal components by a fast Fourier analyzer (Hewlett-Packard, model 5420). The input-power spectrum, cross-power spectrum (input to output), and output-power spectrum were measured and averaged in order to determine the transfer function (impedance) of the preparation.

The fast Fourier analyzer uses a version of the discrete Fourier transform (Brigham, 1974). The analyzer therefore computed the various spectra at evenly spaced frequency points: 256 frequencies between 0 Hz and the maximum frequency selected. Because impedance functions tend to vary exponentially with frequency, the linearly spaced frequency points were converted to a logarithmic scale. In any one data set, such conversion compressed the high frequency and expanded the low frequency points. To have data at a fairly even logarithmic spacing, the data were usually collected in three blocks, from 0 to 25 Hz, from 0 to 400 Hz, and from 0 to 1.6 kHz.[1] These three data sets were then merged into one set of 200 points in the range 0.1–1,600 Hz, selected to be as evenly spaced as possible. Before merging, wild points (which usually occurred at multiples of the line frequency) were removed (see

[1]A fourth data set was often collected over the frequency range of 0 to 6. 4 Hz but in subsequent analysis it was never necessary to use these data.

TABLE I
COMPARISON OF CELLULAR PROPERTIES

Bathing solution	Number of experiments	Stable voltage	G_m^*	G_1^*	ω_1	$G_2^{*\ddagger}$	ω_2	R_e	R_s	SSQ§
		(mV)	*(mS/μF)*	*(mS/μF)*	*(rad)*	*(mS/μF)*	*(rad)*	*(kΩ cm)*	*(kΩ)*	
Normal ± SD	12	−30 ± 4	0.12 ± 0.10	0.04 ± 0.03	4.3 ± 3.1	−0.05 ± 0.04	76 ± 30	20 ± 17	66 ± 53	0.79 ± 0.40
D-600 ± SD	7	−28 ± 7	0.10 ± 0.04	0	—	−0.03 ± 0.02	93 ± 48	17 ± 17	41 ± 54	0.50 ± 0.43
TTX ± SD	4	−27 ± 7	0.17 ± 0.10	0.06 ± 0.02	4.8 ± 3.9	−0.08 ± 0.04	78 ± 48	20 ± 8	47 ± 31	0.73 ± 0.33

*These parameters are normalized by our estimate of specific membrane capacitance C_m. This procedure was adopted because we did not have morphometric data on all of the preparations and the parameters S_m/V_T (surface of membrane/unit volume of tissue) may be variable. See the discussion of *Parameter Values* in Results.

‡G_2 is significantly reduced by D-600. When data from the same cluster were obtained with and without D-600, the ratio of G_2 (with)/G_2 (without) = 0.35 ± 0.28, $n = 5$.

§SSQ (sum-squared error) measures the goodness of fit of our theory to the data.

Mathias et al., 1979, p. 188). Because of limitations imposed by the size of computer core memory that was required for the curve-fitting process, only 200 points in the final data set were used. Since the interesting changes in the impedance curves were nearly complete by 1,600 Hz, the data were truncated at this frequency. Moreover, the signal-to-noise ratio is marginally acceptable at this and higher frequencies.

The final, merged, wild-point-edited and reduced data set was analyzed with a nonlinear curve-fitting routine (see Valdiosera et al., 1974 for further discussion) on a Data General Eclipse S/230 (Data General Corp., Westboro, Mass.). In this procedure, the impedance data , consisting of 200 magnitude points and 200 phase points, were compared with the theoretical predictions from the equations given in Fig. 1 and Eq. 2. The best-fit parameters shown in Tables I, II, or III were determined by minimizing the sum-squared error of datum minus theory.

THEORY

Equivalent Circuit of a Cluster

The equivalent circuit used to describe a cluster is shown in Fig. 1; this circuit is an approximate representation of Eq. 1. The terms that are not included in this equivalent circuit

TABLE II
MORPHOMETRIC PARAMETERS AND SPECIFIC MEMBRANE PROPERTIES IN NORMAL SOLUTION

n = 4	Radius (μm)	$S_m/V_T(cm^{-1})$	V_E/V_T	χ	τ
Mean ± SD	41 ± 7	8,000 ± 600	0.15 ± 0.06	0.81 ± 0.15	1/3 estimated
n = 7	$G_m(mS/cm^2)$	$C_m(\mu F/cm^2)$	$G_1(mS/cm^2)$	$G_2(mS/cm^2)$	$\rho_e(\Omega$ cm)
	0.19 ± 0.19	1.3 ± 0.4	0.07 ± 0.06	−0.08 ± 0.07	65 measured for bath 832 calculated from R_e

*Values expressed as Mean ± SD.

TABLE III

COMPARISON OF CELLULAR PROPERTIES DERIVED USING THE NONUNIFORM SYNCYTIAL MODEL

Bathing solution	Number of experiments	Stable voltage	G_m^*	G_1^*	ω_1	$G_2^{*\ddagger}$	ω_2	r_e	R_s	SSQ§
		(mV)	*(mS/μF)*	*(mS/μF)*	*(rad)*	*(mS/μF)*	*(rad)*	*(Ω cm')*	*(kΩ)*	
Normal ± SD	12	−30 ± 4	0.11 ± 0.10	0.04 ± 0.03	4.3 ± 3.1	−0.05 ± 0.04	77 ± 30	300 ± 300	97 ± 68	0.85 ± 0.42
D-600 ± SD	7	−28 ± 7	0.10 ± 0.04	0	—	−0.03 ± 0.02	91 ± 44	230 ± 210	59 ± 74	0.59 ± 0.43
TTX ± SD	4	−27 ± 7	0.16 ± 0.09	0.06 ± 0.02	4.6 ± 4.1	−0.07 ± 0.04	74 ± 51	610 ± 280	68 ± 37	0.73 ± 0.34

*These parameters are normalized by our estimate of specific membrane capacitance C_m. This procedure was adopted because we did not have morphometric data on all of the preparations and the parameter S_m/V_T (surface of membrane/unit volume of tissue) may be variable. See the disucssion of *Parameter Values* in Results.

‡G_2 is significantly reduced by D-600. When data from the same cluster were obtained with and without D-600, the ratio of G_2 (with)/G_2 (without) = 0.35 ± 0.28, n = 5.

§SSQ (sum-squared error) measures the goodness of fit of our theory to the data.

are $\epsilon\,[U_e(r) + U_e(R)]$, which are induced by the extracellular (intercellular) potential U_e; these will be discussed later.

$$\mathbf{U}_i(\vec{\mathbf{r}}, \vec{\mathbf{R}}) = I \cdot \left\{\frac{1}{4\pi a^2(Y_m + Y_e)} + R_s(\vec{\mathbf{r}}, \vec{\mathbf{R}})\right\} - \epsilon[U_e(r) + U_e(R)], \tag{1}$$

where U_e is described in Eq. 22 of Eisenberg et al. (1979). The other parameters are defined as follows:

$\epsilon = R_i/(R_i + R_e)$ is a small dimensionless parameter.

R_i is the effective intracellular resistivity due to cytoplasm and nexuses (Ω cm).

$R_e = \rho_e/(\tau V_e/V_T)$ is the effective extracellular resistivity due to the small tortuous volume of intercellular spaces (Ω cm).

ρ_e is the specific resistivity of the extracellular solution (Ω cm).

V_e/V_T is the volume of intercellular clefts in a unit volume of tissue.

τ is the tortuosity factor.

a is the cluster radius (cm).

$\vec{\mathbf{r}}$ is the vector describing the location of the voltage recording microelectrode that is r cm from the center of the cluster (cm).

$\vec{\mathbf{R}}$ is the vector describing the location of the current passing microelectrode that is R cm from the center of the cluster (cm).

$Y_m(j\omega)$ is the specific admittance per unit area of membrane. See Eq. 2, (Ω^{-1}/cm^2).

$Y_e(j\omega) = \gamma/R_e\ (\coth \gamma a - 1/\gamma a)$ is the admittance contributed by the radially varying distribution of voltage across the inner membranes, but referred to a unit area of the outer spherical surface (Ω^{-1}/cm^2).

$\gamma(j\omega) = [R_e Y_m(j\omega) S_m/V_T]^{1/2}$ is the propagation coefficient for the intercellular clefts. At dc, γ is one over the length constant (cm^{-1}).

S_m/V_T is the surface area of membrane in a unit volume of tissue, (cm^{-1}).

$j\omega$ is the Fourier transform parameter, where ω is the angular frequency of the applied current sinusoid.

$R_s(\vec{r}, \vec{R})$ is the series resistance due to the point-like source of intracellular current being passed through a microelectrode (Ω).

$I(j\omega)$ is the current applied (A).

These equations and the equivalent circuit are taken from Eisenberg et al. (1979).

All of the membrane in an aggregate is assumed to have uniform specific properties, i.e., the specific admittance, Y_m (Ω^{-1}/cm^2) is the same everywhere. The specific membrane admittance that was used to describe the experimental data was:

$$Y_m(j\omega) = G_m + j\omega C_m + \frac{G_1}{1 + (j\omega/\omega_1)} + \frac{G_2}{1 + (j\omega/\omega_2)}, \tag{2}$$

where G_m and C_m are the conductance and capacitance per unit area of membrane, respectively; the terms involving G_1, ω_1, and G_2, ω_2 represent the linear (potential- and time-dependent) changes in membrane current produced by small perturbations in membrane potential. They are derived in the following section.

The series resistance, R_s, arises from the fact that the cross-sectional area of the path for current flow from a point source (the microelectrode) diminishes as the source is approached. The magnitude of R_s therefore depends strongly on the separation between the potential and current electrodes: the lines of current flow increase in density in proportion to $1/|\vec{r} - \vec{R}|$, so that in principle, R_s could become infinitely large. The exact location of the electrode tips within the preparation could not be determined, however, so that the value of R_s could not be related to that of R_i and the physiological variables that scale its magnitude at any given electrode separation.

One path for current flow out of the preparation is from cell to cell, through gap junctions (nexuses) and cytoplasm, out through cell membrane facing the free outer surface of the preparation to some reference electrode in extracellular space. Most of the potential drop along this path occurs in the immediate vicinity of the source (where the current density is greatest) and at the surface membrane (where the resistance to current flow is greatest). Spatially, the intracellular potential is therefore approximately uniform. This theoretical prediction has been confirmed experimentally by DeHaan and Fozzard (1975) and also below in Results (*The Point Source Series Resistance*), where Fig. 6 shows the change in impedance when the voltage recording electrode is placed far away from the current electrode (A) then near the current electrode (B). The second path for current flow is across inner cell membranes, into the narrow intercellular clefts of extracellular space, and through their openings on the outer surface of the preparation to the reference electrode. This path is represented by the admittance Y_e, which is akin to the input admittance of a cable, the properties per unit length of which vary with length (the radial location in the preparation), i.e., membrane area and cross-sectional area diminish as $1/r$. Because the potential gradients associated with the point-like nature of the source are localized to the near vicinity of the source, Y_e can be considered to be in parallel with the surface membranes, as depicted in the circuit of Fig. 1.

Some terms in Eq. 1 are not represented by this circuit. These terms have the following physical origin. When intracellular current is injected into a cell, the entire intracellular space changes in potential more or less uniformly, driving current into the intercellular clefts.

Because the cross-sectional area of the current pathways in the clefts is small, even small currents produce large radial gradients in cleft potential. Because the cleft membrane current is proportional to $U_i - U_e(r)$, there must be a radial variation in intracellular current corresponding to these changes in cleft membrane current with radial location. The intracellular potential therefore shows a small radial variation which is the negative reflection of the cleft potential, but scaled down by the fraction of cleft space in the tissue, ϵ. To evaluate these terms the location of the electrodes must be known, but this could not be determined with sufficient accuracy in the present experiments. At the frequencies of interest, however, such small variations of intracellular potential were not detected so that the terms in Eq. 1 describing them could be neglected.

Linearization of Nonlinear Conductances

Assume that a channel changes between its conducting and nonconducting state with rate constants that depend on potential:

$$(1 - p) \underset{\beta}{\overset{\alpha}{\rightleftharpoons}} p, \tag{3}$$

where p is the probability of the channel being open, and α and β are potential-dependent rate coefficients for the channel going to the open and closed states, respectively. If the conductance when all the channels are open is g_o, then at any time and potential, the total conductance will be given by

$$g(v,t) = g_o\, p(v,t). \tag{4}$$

Let us identify variations in a quantity with the prefix δ, and mean values with an overscore. For example, if the potential change is a small variation, δv, about an average $\overline{V}$,

$$v(t) = \overline{V} + \delta v(t). \tag{5}$$

If, at the potential $\overline{V}$, the probability $p(\overline{V})$ is > 0 but < 1, the variations in voltage δv will cause variations in the probability function $p(\overline{V} + \delta v,t)$, so that

$$p(\overline{V} + \delta v,t) = p(\overline{V}) + \delta p\,(\delta v,t). \tag{6}$$

The channels that make up the conductance g are presumably selective, so that they will have some electrochemical equilibrium potential, E_o. The total current through these channels is therefore:

$$i(v,t) = [v(t) - E_o]g(v,t). \tag{7}$$

For small variations in potential, the corresponding variations in current are

$$\delta i = \overline{g}\,\delta v + (\overline{V} - E_o)\,\delta g, \tag{8}$$

where

$$\overline{g} = g_o\, p(\overline{V}), \tag{9}$$

and

$$\delta g = g_o\, \delta p. \tag{10}$$

Hodgkin and Huxley (1952) derived a linear differential equation that approximately described the relationship between δp and δv. Chandler et al. (1962) presented the frequency domain admittance function for variations in the current flowing through the conductance $g(v,t)$ due to variations in voltage δv. They presented their results in the following form

$$\delta I(j\omega) = \bar{g}\,\delta V(j\omega) + \frac{G_0}{1 + j\omega/\omega_0}\,\delta V(j\omega), \tag{11}$$

where

$$G_0 = \frac{\partial p(\bar{V})}{\partial v}\,(\bar{V} - E_0)\,g_0, \tag{12}$$

and

$$\omega_0 = \alpha(\bar{V}) + \beta(\bar{V}). \tag{13}$$

The first term on the right hand side of Eq. 11 is linear conductive current flow. The second term arises because of the time dependence of the conductance $g(v,t)$ and has no simple electrical analog.[2]

If two such channels, g_1 and g_2, exist independent of and in parallel with one another, with respective equilibrium potentials, E_1 and E_2, and probabilities of being open, p_1 and p_2, $i(t) = g_1\,p_1(v,t)\,(v - E_1) + g_2\,p_2(v,t)\,(v - E_2)$, then the frequency domain representation of the small variation in current through the parallel combination is:

$$\delta I(j\omega) = (\bar{g}_1 + \bar{g}_2)\,\delta V(j\omega) + \left(\frac{G_1}{1 + j\omega/\omega_1} + \frac{G_2}{1 + j\omega/\omega_2}\right)\delta V(j\omega), \tag{14}$$

and $\bar{g}_{1,2}$, $G_{1,2}$, and $\omega_{1,2}$ are defined analogously with Eqs. 9, 12, and 13.

On the other hand, were there a single channel g_0 whose probability of being open is dependent on the probability of two events occurring simultaneously, each with a different dependence on potential,

$$i(t) = g_0 p_1(v,t) \cdot p_2(v,t)\,(v - E_0), \tag{15}$$

then

$$\delta I(j\omega) = g_0 p_1(\bar{V})\,p_2(\bar{V})\,\delta V(j\omega) + \left(\frac{G_1}{1 + j\omega/\omega_1} + \frac{G_2}{1 + j\omega/\omega_2}\right)\delta V(j\omega). \tag{16}$$

The form of this equation (Eq. 16) is identical to that for the case of two channels in parallel, a linear conductive term and the sum of two probability terms. But now

$$G_1 = g_0 p_2(\bar{V})\,(\bar{V} - E_0)\,\frac{\partial p_1(\bar{V})}{\partial v},$$

$$G_2 = g_0 p_1(\bar{V})\,(\bar{V} - E_0)\,\frac{\partial p_2(\bar{V})}{\partial v}, \tag{17}$$

and $\omega_{1,2}$ are still defined analogously with Eq. 13.

---

[2]Sometimes this term is represented schematically by an inductor in series with a resistor (Fishman et al., 1979; Clay et al., 1979), however, such a representation requires one to allow for negative component values. Furthermore, the physics underlying the phenomena observed here has nothing to do with the time varying magnetic fields in an inductor.

Parallel and series gates can be separated by exploring the potential dependence of the parameters G_1, G_2, ω_1, and ω_2. For example, if G_2 is negative because $\partial p_2/\partial v$ is negative, then the reversal potential E_0 in Eq. 15 must be more negative than $\overline{V}$. Whereas, if G_2 is negative because $\overline{V}$-E_2 is negative, E_2 must be positive to $\overline{V}$.

In summary, G_1 and G_2 are theoretically proportional to the difference between the average membrane potential and an electrochemical equilibrium potential, multiplied by the slope of the steady conductance vs. potential curve evaluated at that average potential. ω_1 and ω_2 each are proportional to the sum of forward and reverse rate constants evaluated at the average membrane potential. Whereas the form of the linearized conductance for series, parallel or second order "gates" is the same, the potential dependence of G_1 or G_2 will differ in these situations, which might permit the kinds of gates to be distinguished from one another.

RESULTS

Aggregates were generally spontaneously active but became temporarily quiesecent after impalement with two microelectrodes. The membrane potential stabilized at an average potential of −28 mV and the input resistance at several megohms. This differs from the behavior described by Clay et al. (1979), where their aggregates stabilized at one of two potentials, either −64m V or −50 mV; see Discussion.

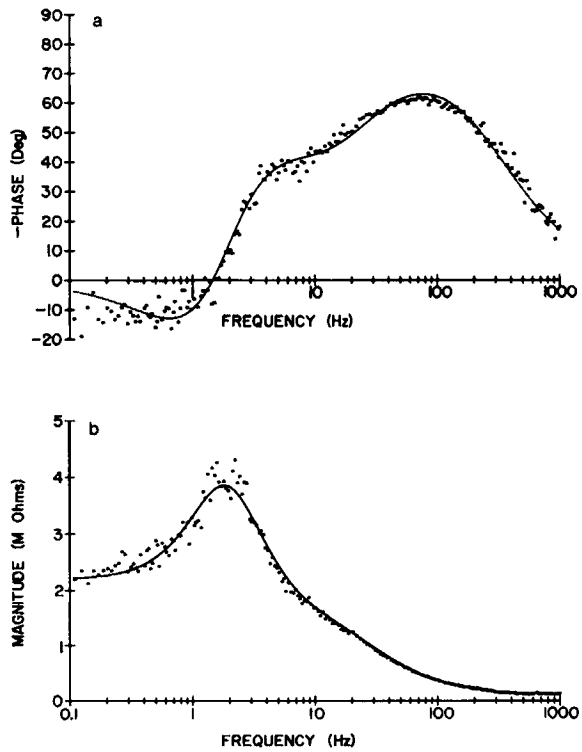

FIGURE 2 The phase angle (*a*) and magnitude (*b*) obtained from a cluster, untreated with any pharmacological agents. The solid line is the best-fit theoretical curve generated by the circuit of Fig. 1. The stable membrane potential was −26 mV.

Aggregate Impedance

The impedance data shown in this section were collected by impaling an aggregate with two microelectrodes; one electrode passed small stochastic currents and the other measured the resulting stochastic displacements in membrane potential. The smooth curve passing through the data is the best fit of a theoretical curve generated from the circuit in Fig. 1.

Fig. 2 shows the magnitude and phase angle for the impedance of an aggregate in the absence of any pharmacological agents. The magnitude function measures the input "resistance" of the preparation to a sinusoidal current at a given frequency. The magnitude of the impedance rose precipitously around 2 Hz, which indicates that a small current at this frequency would produce an extraordinarily large change in potential. The mechanism underlying this resonance peak may be related to pacemaker activity, since the aggregates beat spontaneously at about the same frequency. We have no direct evidence, however, for such a relationship.

The phase angle is simply the normalized time delay betwen a peak in the sine wave of injected current and the corresponding peak in the induced displacement of potential. At low frequencies, the phase function fell below the axis, which indicates phase lead, such lead being a consequence of G_1 and ω_1 of Eq. 2 (for values see Table I). As the frequency increased, the phase angle rapidly crossed the axis, becoming phase lag, to reach a rather sharp peak at 5

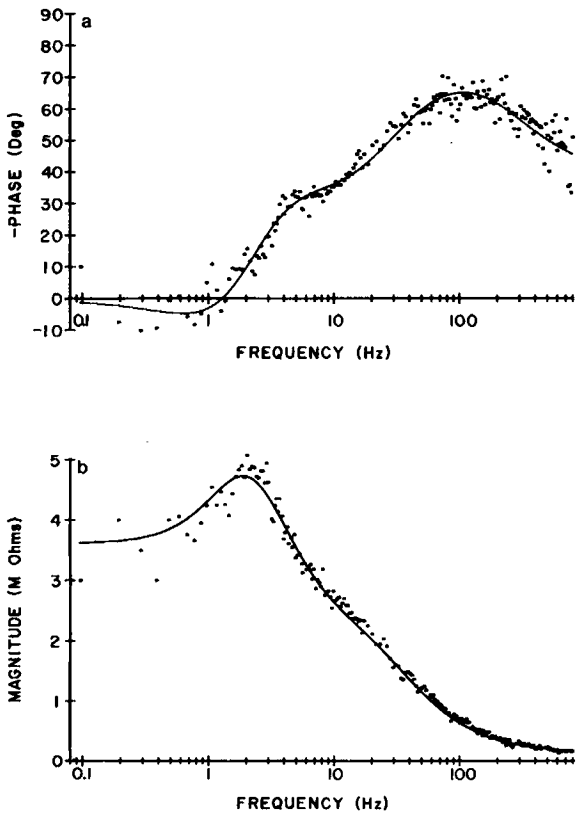

FIGURE 3 The phase (*a*) and magnitude (*b*) from a cluster treated with TTX. The stable membrane potential was −29 mV.

Hz. This rapid increase and peak in the phase were most directly related to G_2 and ω_2. At higher frequencies, the membrane current became almost entirely capacitive and the magnitude of the displacement in transmembrane potential approached zero. The series resistance arising from the point-like nature of the current source then dominated the impedance to current flow, the phase angle declining to zero as the magnitude approached, asymptotically, the value of R_s.

The impedance data illustrated in Fig. 3 were from an aggregate treated with 100 mg/liter of tetrodotoxin (TTX). The data in Figs. 2 and 3 appear similar and, on the average, the circuit parameters in Table I determined from aggregates with or without TTX were not significantly different. Certainly, TTX had no substantial effect on the resonant behavior.

The impedance data in Fig. 4 were collected during one impalement of one aggregate in the presence and absence of D-600 (1.25 mg/liter). The peak in the magnitude plot and the peak and lead in the phase plot observed in the absence of the drug were greatly reduced when the drug was added, the impedance being now reasonably well described by a membrane model in which G_1 and G_2 of Eq. 2 were almost zero. Except for reducing G_1 and G_2, D-600 seemed to have no significant effect on the circuit parameters of Table I.

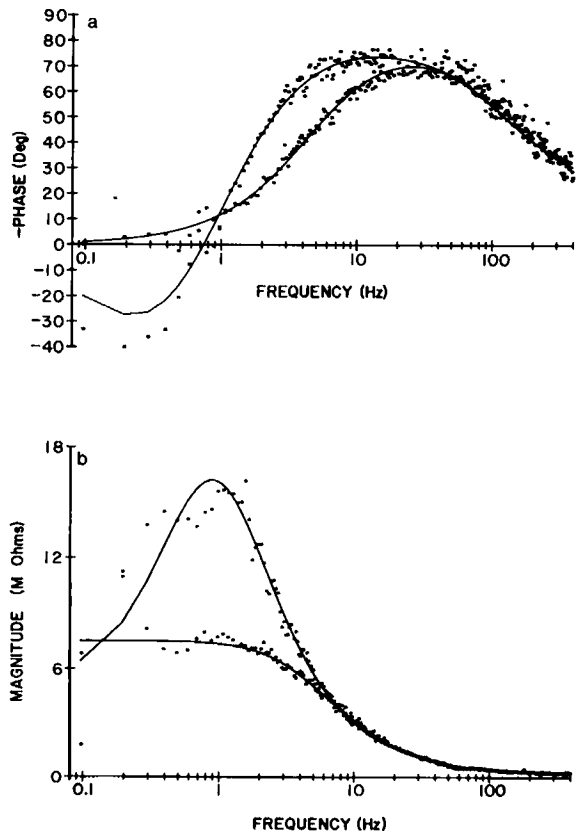

FIGURE 4 The phase angle (*a*) and magnitude (*b*) of a cluster before and after treatment with D-600. The theoretical curves were computed with the same circuit parameters except, in D-600, the values of $G_1 = G_2 = 0$ for this cluster.

Parameter Values

The smooth curves going through the data in Figs. 2–4 were derived by varying the circuit parameters in Table I until a best fit was obtained. The average circuit parameter values derived from a number of different impedance data sets are presented in this table. The only pharmacological intervention tested that had a statistically significant effect on any parameter was D-600, which blocked the ionic currents that gave rise to G_1 and G_2.

In three experiments, we were able to obtain morphometric and impedance data from the same clusters. The specific circuit parameters derived from these clusters, and several other impedance experiments on the same batch of clusters, are presented in Table II. The expression for the extracellular admittance $Y_e(j\omega)$ given in Theory or in Fig. 1 contains only the volume membrane admittance $Y_m(j\omega)\, S_m/V_T$. Thus, electrical measurements alone cannot determine the specific membrane admittance $Y_m(j\omega)$; to determine $Y_m(j\omega)$ one must independently measure S_m/V_T. Many of the experiments reported in Table I were performed almost one year after those in which morphometric analysis was included. When curve-fitting the later experiments, if S_m/V_T was fixed at the earlier measured value, all of the membrane parameters scaled down by a factor of ~ 54%, which indicates that the average value of S_m/V_T had probably changed. When specific membrane conductances G_m, G_1, and G_2 were referred to the value of specific membrane capacitance, C_m, the change in parameter values disappeared, and indeed the variance also was reduced. Because C_m is likely to be near $1\mu F/cm^2$, we believe that this normalization provides our best estimate of true membrane conductance, particularly in the absence of an independent morphometric on measurement of S_m/V_T.

Linearity

Because the resonance arises, in all likelihood, from inherently nonlinear ionic currents, it was important to determine whether the perturbations in membrane potential were in the linear range. One test of nonlinearity is built into the Fourier analyzer; it is the coherence function (see Mathias et al. [1979] for a precise definition of coherence). Unfortunately, the coherence function is an insensitive indicator of nonlinearity, whereas it is very sensitive to the signal-to-noise ratio. A more stringent test for linearity is to show that impedance is independent of the amplitude of the current. In a linear system, if the input is tripled, the output should triple, the impedance (i.e., the ratio of output/input) remaining unchanged. Fig. 5 illustrates the magnitude of the impedance function for two data sets from the same aggregate. The curve in Fig. 5*A* was generated by approximately tripling the input current used to obtain the curve of Fig. 5*B*. The curve of 5*B* is noiser than that of 5*A*, since the signal-to-noise ratio was less in *B* than in *A*. If, however, the curve in 5*A* is subtracted from the curve in 5*B*, the result is nearly a zero mean, which indicates only a small deviation from linearity between the two current strengths (see panel 5*C*). Thus, at the current levels we used there is no reason to doubt the assumption of linearity.

The Point Source Series Resistance

The series resistance R_s is an inescapable consequence of the point-like nature of a microelectrode as a current source and will always be part of an equivalent circuit of the preparation whenever such a source is used. The magnitude of R_s depends both on the distance separating the current and potential-recording electrodes, and on the geometry of the tissue or

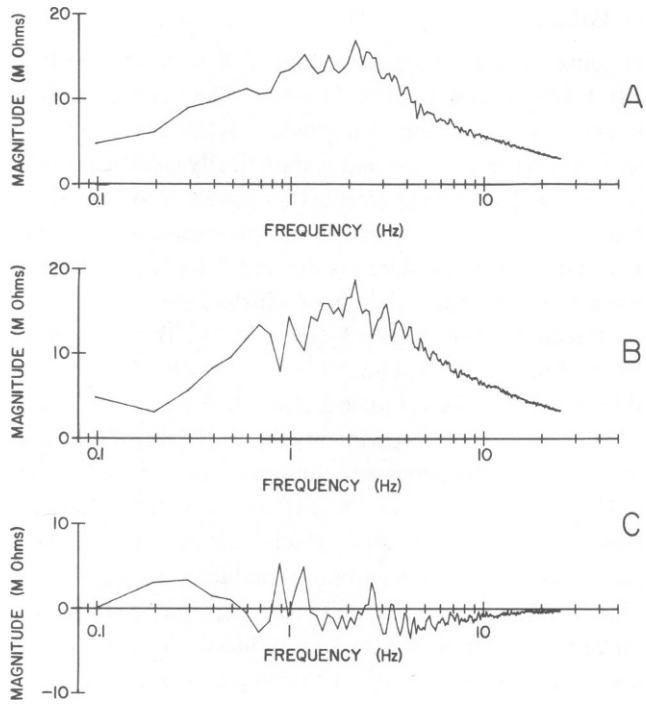

FIGURE 5 Magnitude data obtained at different levels of input current together with the residual nonlinear difference curve. *A*, magnitude data from the impedance function of an aggregate obtained with an unusually high level of injected current. *B*, the "same" data obtained a few minutes later with the usual level of current, ~ 1/3 less than that in *A*. *C*, the difference between curves *A* and *B*. In a linear system, the difference should be zero mean.

cell. In preparations in which one dimension predominates, such as a cylindrical cell, except for the immediate vicinity of the current source (within a distance roughly equal to the overall diameter), one is sufficiently far away from the source to escape the effects of its point-like nature (see Eisenberg and Johnson, 1964). In a spherical tissue, however, since one is constrained to record the voltage within a diameter away from the current source, the point source effect can never be neglected. This origin of R_s was demonstrated by the results of an experiment in which two impedance data sets were recorded from the same aggregate for two different electrode separations (see Fig. 6). The only difference in the two sets of theoretical curves is in the value of R_s. This experiment also demonstrates the approximate spatial uniformity of the intracellular voltage, except for the point source effect. That R_s is indeed due to the point source and not to either the bath resistance or to a layer of fibroblasts that surround an aggregate was demonstrated by moving both electrodes out of the cells into the extracellular space within the aggregate, in which case the residual series resistance could not be measured with high resistance microelectrodes and was therefore at least one order of magnitude less than the point-source effect.

Nonuniformities in the Extracellular Space

In other tissues, the volume fraction of extracellular space observed in the electron microscope has been nearer to the electrically determined number for that space. The volume measured

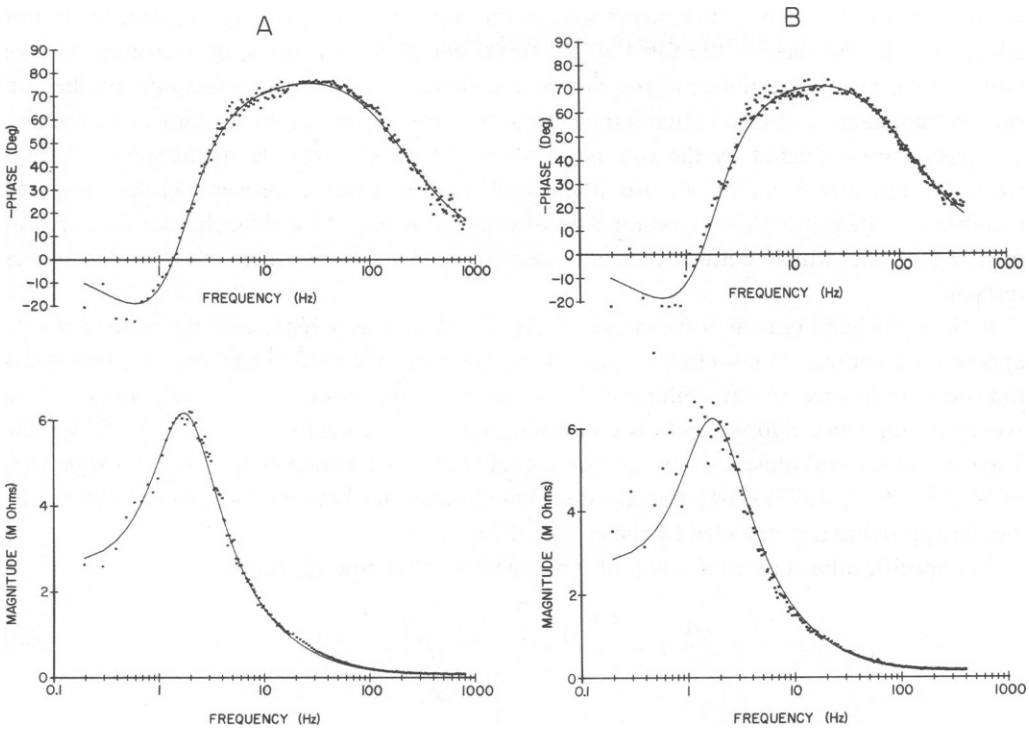

FIGURE 6 Demonstration that the series resistance, R_s, originates from the point-like nature of the current source. The circuit parameters for the cluster were determined from the data in panel A. The data in panel B were obtained from the same cluster but with the potential measuring electrode much closer to the current electrode. The theorectical curves in panel B were generated with the parameter values determined from panel A data, except the value of R_s was increased. In panel A, R_s = 67 kΩ; in panel B, R_s = 135 kΩ. This change in R_s can be seen as the change in high frequency asymptote for the magnitude function. Clearly, R_s represents a small percentage of the total input resistance, so that the intracellular voltage is nearly spatially uniform.

by Mobley and Eisenberg (1976) for the tubular system of frog skeletal muscle was used by Mathias et al. (1977) to estimate from their impedance data the resistivity of the solution within the tubules. The value of resistivity thus obtained was the same order of magnitude of that for Ringer's solution. Moreover, Mathias et al. (1979) used the volume measured by Yorio and Bentley (1976) for the volume of intercellular space between the cells of the lens, and found that the resistivity of the solution filling this space was near to that of Ringer's solution.

The membranes within an aggregate may be separated into two almost equally probable categories: closely apposed and not closely apposed. The closely apposed membranes include not only those that form junctional complexes (nexuses, desmosomes, fasciae adherentes), but also those regions where the cells are packed together and flattened. Rather than conclude that in some preparations the resistivity of the extracellular fluid is much higher than that of tissue-culture medium, one must recognize that extracellular space within the cluster is not uniformly distributed. The majority of extracellular space lies as a thin shell beneath an outer nonmuscle shell and an inner muscular core where extracellular space is sparsely distributed.

A considerable fraction of the membrane of the muscle cells is closely apposed to that of adjacent cells, not only in the form of junctional complexes (nexuses, desmosomes, fasciae adherentes), but where the cells are packed together and flattened against one another. In such circumstances, electron microscopic measurements of the volume fraction of extracellular space are dominated by the volume between not closely apposed membranes, whereas electrical measurements of R_e are dominated by the volume between closely apposed membranes. Such morphology requires an alternative to Eq. 2 for describing a unit area of membrane, one which defines internal membranes that have either high or low series resistance.

In the right-hand branch of the circuit of Fig. 7 a parameter χ represents the ratio of closely apposed membranes to not closely apposed membranes. A specific resistance, r_a, represents the access resistance of extracellular clefts between membranes that are closely apposed (see Appendix for more rigorous details concerning r_a). An analogous situation prevails for the T-system in skeletal muscle where a "disk model" analysis (Adrian et al., 1969, an appendix, or Mathias et al., 1977) shows that the distributed resistance between two disks of membrane can be approximately modeled by the circuit of Fig. 7.

The specific admittance for a unit of inner membrane is now Y_m^*, where

$$Y_m^* = \frac{1}{1+\chi} Y_m + \frac{1}{r_a + \frac{1}{Y_m}} \left(\frac{\chi}{1+\chi} \right). \tag{23}$$

This nonuniform access model of a cell aggregate is completed by substituting Y^*_m for Y_m in the equation for Y_e, the extracellular admittance of Fig. 1. In considering the fitting of impedance data to this new model, it can be seen that there are two additional parameters, χ and r_a. Because it was desirable to keep the number of variable parameters to a minimum during the curve-fitting procedure, the parameter χ was set to its average value, as determined from morphometric measurements. The parameter R_e was set to a value estimated from morphometric measurements of average extracellular volume, on the assumption that

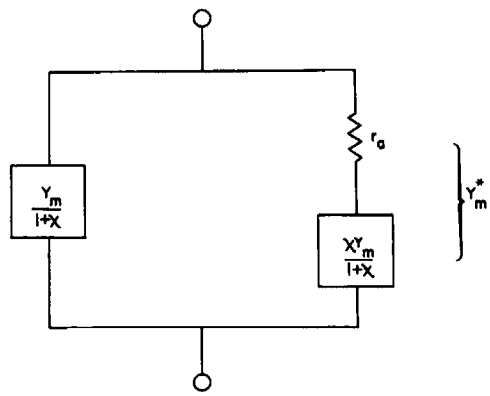

FIGURE 7 The nonuniform access model of a unit area of membrane. This model assumes that the membrane of the preparation exists in two forms: closely apposed and not closely apposed, where χ = (area of closely apposed)/(area of not closely apposed). The parameter r_a is the access resistance to the regions of closely apposed membranes; its morphometric dependencies are outlined in the appendix.

the not closely apposed extracellular space is filled with tissue-culture solution. With these assumptions, the number of variable parameters in the nonuniform model was the same as that in the standard syncytical model; in the nonuniform model, the parameter r_a was varied, whereas in the standard model, the parameter R_e was varied. In the standard model, however, when there are extracellular nonuniformities, there is no direct relation between R_e and structure, whereas the nonuniform model provides a direct relation between R_e and structure. The nonuniform model is superior in the sense that it allows us to put a constraint of reasonableness on the value of r_a (see the appendix, which relates r_a to structure), on the basis of the structural measurements from electron microscopic studies. The sum-squared error of the nonuniform access curve fits, SSQ in Table III, is no different from the SSQ for a standard fit listed in Table I, and the membrane parameters are essentially identical for both models. The theoretical curves shown in the figures are therefore from the standard model. The probable reason for the wide variation in r_a (R_e) is discussed later (see Discussion).

DISCUSSION

Variability of Parameters

The variations observed in the data in Tables I and III can be ascribed not only to inherent variability in the measured parameters, but also to the fact that the more parameters that must be used to account for an experimental observation, the less well determined is the numerical value of each parameter. Our procedure has always been to include every parameter that must, from a stuctural point of view, be present (Eisenberg and Mathias, 1980). Every biological membrane must have a capacitance due to the oil film, and a conductance due to channels or diffusion of ions across the oil film. In addition, every tissue must have electrical properties conferred by the geometry of current flow and the finite resisitivity of intra- and extracellular space. In our experiments on heart muscle, however, there are more processes present than those just listed. Four new parameters, $G_{1,2}$ and $\omega_{1,2}$ were required to account for the resonance in the magnitude of the impedance data and the complex behavior of the phase angle. These inclusions, in themselves, ensure each derived parameter value will have more variance. In the presence of D-600, when the effect of nonstructural parameters was minimized, the average values for structural parameters were essentially the same as those determined in the absence of the drug. Thus, our average parameter values do not appear to have been biased by the inclusion of the parameters describing the two active currents.

Comparison with Other Results

Our average value of specific membrane resistance, R_m, at a transmembrane potential of -28 mV, is ~ 8 kΩ cm^2. This is somewhat lower than the values of specific resistance reported for heart muscle at more hyperpolarized potentials (Mobley and Page, 1972; Lieberman et al., 1975); the difference in stable potentials is probably a sufficient explanation for this finding. Another possibility, that leaks were induced at the site of impalement, seems unlikely since the resultant potential would not be expected to remain steady for the 20 min required for a complete experimental run.

Our value of specific capacitance of 1.3 μF/cm^2 is also higher than one expects for a biomembrane. The morphometric studies included in this paper are certainly not exhaustive

and if our value of surface of inner membrane per unit volume of tissue, $S_m/V_T = 8{,}000\ \text{cm}^{-1}$, were too small, our estimate of specific capacitance would be too large.

Stable Membrane Voltage

The magnitude of the "resting" potential in a tissue that normally pacemakes differs in its significance from that of a normally quiescent cell, where it is usually viewed as measuring the health of the preparation and quality of impalement. Often the quiescent potential can be switched between two stable values simply by briefly passing current (Clay et al., 1979). Other investigators (Lee and Fozzard, 1979) found that low extracellular K^+ concentration caused sheep Purkinje fibers to depolarize to a stable voltage of ~ -40 mV. An input resistance consistent with a specific membrane resistance of reasonable value and stability of the quiescent potential were therefore judged better criteria for a successful impalement than the magnitude of the quiescent potential. The difference in quiescent potentials reported by Clay et al. (1979) and those reported here may result from differences in the culture process.

Further Investigation

The values we report for R_s include the effects of electrode position, cytoplasmic resistivity, and cell-to-cell coupling. Although it is possible to use the measurement of point source resistance, R_s, as a measure of cell-to-cell coupling (Mathias et al., 1981), the relative position of the microelectrodes within the preparation must be determined, a frequently difficult if not impossible task. When used as a measure of changes in cell-to-cell coupling, however (as a result of an intervention, for example), such careful localization is not required. Although this use of R_s to study cellular communication has not yet been exploited, the small spherical shape of the heart cell clusters and the resulting large value of R_s make such experiments now feasible.

The parameters describing the nonlinear slow currents in heart muscle need to be studied at different steady membrane voltages. This could be accomplished by performing small signal-impedance studies on top of voltage-clamp steps. If the voltage dependence of G_1, G_2, ω_1, and ω_2 were mapped, and if our view of the molecular events underlying these parameters is correct, the nonlinear, time- and voltage-dependent conductances could be reconstructed, theoretically, from the linear, frequency domain data. We also need to determine the ionic selectivity of G_1 and G_2 and indeed, the physiological role of these currents.

Although no difference in ultrastructure was observed between preparations with negligible and large values of R_e, the reason for the variation in R_e from preparation to preparation might still lie in a variation in the fine structure of extracellular space within the muscular core of the preparation. Morphometric measurements show that the small fraction of extracellular space within the muscular core occurs as small scattered dilation of the narrow extracellular clefts between closely apposed cells. In some preparations, these small dilations might represent invaginations of the outer shell of extracellular space, whereas in others they might represent isolated pockets effectively isolated, electrically, from the outer shell. Such an hypothesis could be tested by marking extracellular space with the horseradish peroxidase reaction and by reconstructing extracellular space, three-dimensionally, from stereomicrographs of thick sections viewed inhe high-voltage electron microscope.

Implications for Voltage-clamp Studies

Two parameters of considerable interest during assessment of the suitability of a preparation for voltage clamp are the series resistance, R_s, and the effective extracellular resistivity, R_e. R_s must be compensated for (e.g., by positive current feedback [Hodgkin and Huxley, 1952]) in order to have rapid control of potential in voltage clamp. R_e is a measure of the radial variation in extracellular (cleft) potential, and if this parameter is large, the necessary spatial uniformity of transmembrane potential cannot be obtained. The length constant for potential changes in the extracellular space is $\sim 1/(R_e G_m S_m/V_T)^{1/2}$, so that an estimate of the degree of spatial uniformity can be obtained by substituting the peak value of the potential-dependent ionic conductance as G_m and comparing the resulting length constant with the radius of the preparation. As can be seen from Table I, R_e varies considerably from preparation to preparation: in about one-third of the preparations studied it could not be distinguished from zero, as would be expected were the extracellular space evenly distributed throughout the muscular core of the preparation. Using the average extracellular volume fraction of 14% given in Table II and including the effect of tortuosity (see Table II), we estimate that the average effective extracellular resistivity would be $\sim$ 1,000 Ω cm, assuming that the extracellular volume was filled with culture medium. Our resolution was, however, probably about 2,000 Ω cm, since a change in R_e of this magnitude was required in order to produce a noticeable change in the theoretical impedance curves. On the assumption of a value of 2,000 Ω cm for those preparations in which R_e could not be distinguished from zero, a successful clamp of the peak sodium current would be possible, at least from holding potentials at which the conductance was partially inactivated.

In the majority of preparations, however, R_e was found to be $>$ 2,000 Ω cm, reaching as high as 40,000 Ω cm in some preparations. These findings are consistent with the experimental observations of Ebihara et al. (1980), who found that the fast sodium current could be successfully analyzed by voltage clamp only in a small fraction of the clusters penetrated.

The size of the preparation was apparently not a factor determining the value of the volume resistivity R_e (r_a), since preparations of equally small size could have either a negligible or a large value. This is of course what one would expect since R_e is a resistivity. The total resistance in series with an inner membrane located near the center of the cluster will depend on both R_e and radius. Thus, it is generally true that smaller clusters are preferable when voltage-clamp studies are performed.

Summary and Conclusions

Tissue-cultured spherical clusters of embryonic chick heart cells have membrane properties that resemble those of other cardiac muscle. Although the spherical geometry, small size, and large extracellular space make this preparation relatively well suited for voltage-clamp analysis of the fast inward current in heart muscle, the variable packing of the cells requires one to select carefully those preparations that have negligible values of R_e. Although most clusters would be poor candidates for fast voltage-clamp analysis of membrane currents, in any culture dish there will be a few preparation that are, in this regard, superior to most naturally occurring tissue. The identification of a good candidate is a serious practical problem. Obviously, the smallest clusters are potentially the best candidates, but one cannot know if the clamp has been successful until analysis of the data is complete.

The linear impedance studies performed at a stable membrane voltage of −30 mV indicate that tissue-cultured clusters possess many of the interesting ionic currents present in naturally occurring preparations of cardiac muscle. R. Levis (personal communication) has obtained impedance data from sheep Purkinje fibers at a stable voltage of −30 mV that exhibit resonant behavior almost identical to that observed in the clusters studied here. The ability to extract parameter values describing nonlinear, voltage-dependent currents, from linear, frequency-domain impedance analysis, promises an interesting new technique for the study of slow currents in heart muscle.

APPENDIX

The nonuniform access model for a unit area of membrane, shown in Fig. 6 of the text can be directly related to the structure of a heart cell cluster. Assume that the closely apposed membranes are pushed together at a disk of average radium ξ. The admittance of such a disk is given by

$$Y_d = 2\pi\,\xi\left(\frac{2Y_m}{r_e}\right)\frac{\tfrac{1}{2}\,I_1\left(\sqrt{r_e 2\,Y_m}\,\xi\right)}{I_0\left(\sqrt{r_e 2\,Y_m}\,\xi\right)}\,\Omega^{-1}, \tag{A1}$$

where Y_m is the specific membrane admittance described by Eq. 2 of the text.

$$r_e = \rho_e/d, \tag{A2}$$

where d is separation of closely-apposed membranes (cm), and ρ_e is the resistivity of the solution between closely-apposed membranes (Ω cm). The functions $I_0(z)$ and $I_1(z)$ are hyperbolic Bessel functions of the complex argument z.

The general form of Eq. A1 is derived in an appendix to Adrian et al. (1969); a more specific derivation that uses the dimensions of the disk is presented in Mathias (1975). If we wish to convert Eq. A1 into units of specific admittance, that is, the admittance per square centimeter of membrane within the disk, we divide by $2\pi\xi^2$, where the factor of 2 arises because there are two sides of membrane in the disk. Only a fraction (χ) of each unit area of membrane in a cluster is associated with closely apposed regions; therefore, if we want to know the admittance per unit area of cluster inner membrane, we must include properly scaled admittances for both closely apposed and not closely apposed membranes, viz

$$Y_m = \frac{1}{1+\chi}\,Y_m + \frac{\chi}{1+\chi}\,\frac{Y_d}{2\pi\xi^2}. \tag{A3}$$

In general, the distributed admittance, Y_d, can be represented by a lumped circuit if the arguments for I_0 and I_1 are small (Adrian et al., 1969). The lumped circuit limit simply means that there is little radial decrement in the voltage between the disks. The derivation of the syncytial theory of current flow (Eisenberg et al., 1979) is based on the premise that voltage changes over the distance of a few cells is small. Because each disk of radius ξ is assumed to be similar to the dimensions of a cell, we must, if our analysis is appropriate, always be in the limit where a lumped circuit approximation for Y_d is appropriate. If we apply this limit, Eq. A3 becomes

$$Y_m^* = \frac{1}{1+\chi}\,Y_m + \frac{1}{\left(\frac{\rho_e\xi^2}{4d}\right)+\left(\frac{1}{Y_m}\right)}\,\frac{\chi}{1+\chi}. \tag{A4}$$

If we compare Eq. A4 to the circuit in Fig. 6, we see that

$$r_a = \rho_e\,\xi^2/4d. \tag{A5}$$

The access resistance, r_a, is therefore related to structural parameters, but the strucutral parameters in Eq. A5 are microscopic in nature rather than macroscopic like S_m/V_T or V_e/V_T, and may therefore be subject to more variability.

The authors wish to thank Dr. W. J. Adam, Ms. P. Bullock, and Mr. O. W. Oakeley for their technical assistance. We should also like to thank Dr. R. S. Eisenberg for his support, advice, and careful reading of the manuscript.

This research was supported in part by grants HL 12157, GM07184, HL07101, HL20230 from the National Institutes of Health, and American Heart Association grant 79-851 with funds contributed in part by the Chicago Heart Association.

Received for publication 15 October 1980 and in revised form 18 March 1981.

REFERENCES

Adrian, R. H., W. K. Chandler, and A. L. Hodgkin. 1969. The kinetics of mechanical activation in frog muscle. *J. Physiol. (Lond.).* 204:207–230.

Bezanilla, F., and C. M. Armstrong. 1975. Properties of the sodium channel gating current. *Cold Spring Harbor Symp. Quant. Biol.* 40:297–304.

Brigham, E. O. 1974. The Fast Fourier Transform. Prentice-Hall, Inc., Englewood Cliffs, N.J.

Chandler, W. K., R. FitzHugh, and K. S. Cole. 1962. Theoretical stability properties of a space-clamped axon. *Biophys. J.* 2:105–127.

Chen, Y. 1979. On the admittance of membranes associated with channel conduction. Application to channels at nonequilibrium steady state. *J. Theor. Biol.* 81:633–644.

Clay, J. R., L. J. DeFelice, and R. L. DeHaan. 1979. Current noise parameters derived from voltage noise, and impedance in embryonic heart cell aggregates. *Biophys. J.* 28:169–184.

Colatsky, T. J., and R. W. Tsien. 1979 Sodium channels in rabbit cardiac Purkinje fibers. *Nature (Lond.).* 278:265–268.

DeHaan, R. L., and H. A. Fozzard. 1975 Membrane response to current pulses in spheriodal aggregates of embryonic chick heart cells. *J. Gen. Physiol.* 65:207–222.

Ebihara, L., N. Shigeto, M. Lieberman, and E. A. Johnson. 1980. The initial inward current in spherical clusters of chick embryonic heart cells. *J. Gen. Physiol.* 75:437–456.

Eisenberg, R. S., V. Barcilon, and R. T. Mathias. 1979. Electrical properties of spherical syncytia. *Biophys. J.* 25:151–180.

Eisenberg, R. S., and R. T. Mathias. 1980. Structural analysis of electrical properties. *Crit. Rev. Bioeng.* 4:203–232.

Falk, G., and P. Fatt. 1964. Linear electrical properties of striated muscle fibers observed with intracellular electrodes. *Proc. R. Soc. Lond. B Biol. Sci.* 160:69–123.

Fishman, H. M., D. Poussart, and L. E. Moore. 1979. Complex admittance of Na^+ conduction in squid axon. *J. Membr. Biol.* 50:43–63.

Hodgkin, A. L., and A. F. Huxley. 1952. A quantitative description of membrane current, and its application to conduction, and excitation in nerve. *J. Physiol. (Lond.).* 117:500–544.

Horres, C. R., M. Lieberman, and J. E. Purdy. 1977. Growth orientation of heart cells on nylon monofilament. Determination of the volume to surface area ratio and intracellular potassium concentration. *J. Membr. Biol.* 34:313–329.

Johnson, E. A., and J. R. Sommer. 1967. A strand of cardiac muscle: its ultrastructure, and the electrophysiologic implications of its geometry. *J. Cell Biol.* 33:103–129.

Lee, C. O., and H. A. Fozzard. 1979. Membrane permeability during low potassium depolarization in sheep cardiac Purkinje fibers. *Am. J. Physiol.* 273:C156–C165.

Lee, K. S., R. Kao, T. Weeks, N. Akaike, and A. M. Brown. 1979. Sodium current of single cardiac muscle cells. *Biophys. J.* 25:67*a*. (Abstr.)

Lieberman, M., T. Sawanobori, J. M. Kootsey, and E. A. Johnson. 1975. A synthetic strand of cardiac muscle. Its passive electrical properties. *J. Gen. Physiol.* 65:527–550.

Lieberman, M., T. Sawanobori, N. Shigeto, and E. A. Johnson. 1976. Physiologcial implications of heart muscle in tissue culture. *In* Developmental, and Physiological Correlates of Cardiac Muscle. M. Lieberman, and T. Sano, editors. Raven Press, New York. 139–154.

Mathias, R. T. 1975. A study of the electrical properties of the transverse tubular system in skeletal muscle. Dissertation, University of California at Los Angeles.

Mathias, R. T., R. S. Eisenberg, and R. Valdiosera. 1977. Electrical properties of frog skeletal muscle fibers interpreted with a mesh model of the tubular system. *Biophys. J.* 17:57–93.

Mathias, R. T., J. L. Rae, and R. S. Eisenberg. 1979. Electrical properties of structural components of the crystalline lens. *Biophys. J.* 25:181–201.

Mathias, R. T., J. L. Rae, and R. S. Eisenberg. 1981. The lens as a nonuniform syncytium. *Biophys. J.* 34:61–83.

Mobley, B. A., and E. Page. 1972. The surface area of sheep cardiac Purkinje fibres. *J. Physiol. (Lond.).* 220:547–563.

Mobley, B. A., and B. R. Eisenberg. 1975. Sizes of components in frog skeletal muscle measured by methods of stereology. *J. Gen. Physiol.* 66:31–45.

Morad, M., and G. Salama. 1979. Optical probes of membrane potential in heart muscle. *J. Physiol. (Lond.).* 292:267–295.

Nathan, R. D., and R. L. DeHaan. 1979. Voltage clamp analysis of embryonic heart cell aggregates. *J. Gen. Physiol.* 73:175–198.

Schneider, M. F. 1970. Linear electrical properties of the transverse tubules and surface membrane of skeletal muscle fibers. *J. Gen. Physiol.* 56:640–671.

Valdiosera, R., C. Clausen, and R. S. Eisenberg. 1974. Impedance of frog skeletal muscle fibers in various solutions. *J. Gen. Physiol.* 63:460–491.